

SPACE CHARGE EFFECT IN LOW ENERGY MAGNETIZED ELECTRON BEAM*

S. A. K. Wijethunga†, J. R. Delayen, G. A. Krafft¹
Old Dominion University, Norfolk, Virginia, 23529, USA

M. A. Mamun, R. Suleiman, M. Poelker, S. Zhang, J. Benesch

Thomas Jefferson National Accelerator Facility, Newport News, Virginia, 23606, USA

¹ also at Thomas Jefferson National Accelerator Facility, Newport News, Virginia, 23606, USA

Abstract

Magnetized electron cooling is one of the major approaches towards obtaining the required high luminosity in the proposed Electron-Ion Collider (EIC). In order to increase the cooling efficiency, a bunched electron beam with a high bunch charge and high repetition rate is required. At Jefferson Lab, we generated magnetized electron beams with high bunch charge using a compact DC high voltage photo-gun with bialkali antimonide photocathode and a commercial ultra-fast laser. This contribution discusses how magnetization affects space charge dominated beams as a function of magnetic field strength, gun high voltage, and laser pulse width, and spot size in comparison with simulations performed using General Particle Tracer (GPT).

INTRODUCTION

The proposed EIC must provide high luminosity to achieve the promised physics goals and this necessitates small transverse emittance at the collision point. Emittance growth can be reduced by the process called electron cooling. The cooling rate can be significantly improved using a “magnetized electron beam” where this process occurs inside a solenoid field [1, 2]. However, the fringe radial magnetic field at the entrance of the solenoid creates a large additional rotational motion which adversely affects the cooling process inside the solenoid. In order to overcome this effect, the electron beam is created inside a similar field but providing a rotating motion in the opposite direction, so that the fringe field effects at the exit of the photo-gun and at the entrance of the cooling solenoid exactly cancel.

In order to have efficient cooling, the cooling electron beam must have high bunch charge, high repetition rate, and low temperature (i.e., low emittance and low energy spread). These features combine into enhancing the collective interactions, such as space charge effect. A series of measurements were carried out to study the space charge effect in magnetized electron beam particularly, how magnetization affect the space charge current limitation as a function of gun high voltage, laser pulse width and laser

spot size. Simultaneously, GPT simulations were performed. This paper presents a detailed version of the simulations in comparison with the measurements which can be used to optimize the parameters for better results.

MAGNETIZED ELECTRON SOURCE

The experimental beamline consists of photo-gun high voltage chamber, photocathode preparation chamber, cathode solenoid, laser system, three fluorescent YAG screens, four focusing solenoids and beam dump. A schematic diagram of the beamline is shown in Figure 1.

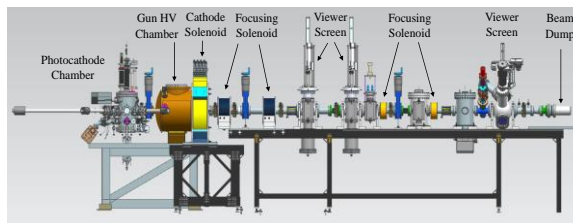


Figure 1: The diagnostic beamline.

The compact gun high voltage chamber includes an inverted insulator and spherical cathode electrode operating at or below -225 kV. The cathode-anode gap is 9 cm and the anode aperture is 1 cm in radius. A bialkali antimonide (K2CsSb) photocathode deposited on GaAs substrate was used with full active area of 6 mm radius and quantum efficiency (QE) of 5-8% with 523 nm laser. A commercial ultra-fast laser with pulse duration less than 0.5 ps, 20 μ J pulse energy, operating at 50 kHz pulse repetition and 1030 nm wavelength (NKT Origami) was used as the laser source for the experiment. The IR beam was converted to 515 nm using a BBO crystal. The laser spatial and temporal profiles were Gaussian. To explore the parameter space, the laser beam spot size at the photocathode was varied by changing a focusing lens and the temporal pulse width was varied using a pulse stretcher built with diffraction gratings [3]. The magnetic field at the photocathode was provided by a solenoid magnet designed to fit at the front of the gun chamber, 0.21 m from the cathode. The magnet operates at a maximum current of 400 A to provide up to 0.1514 T at the photocathode. The diagnostic beam line extends to 4.5 m from the photocathode with different beam pipe aperture sizes from 1-5 cm in radii. Additionally, there are several steering dipole magnets and four focusing solenoids located at 0.49, 1.01, 2.35, and 2.94 m along the beamline.

* Authored by Jefferson Science Associates, LLC under U.S. DOE Contract No. DE-AC05-06OR23177. Additional support comes from Laboratory Directed Research and Development program.

† wwije001@odu.edu

THEORETICAL BACKGROUND

The magnetic field at the cathode can generate canonical angular momentum, which in effect increases the total emittance of the electron beam [4]. Thus, for a magnetized electron beam, the transverse size is set by the beam's correlated emittance which is much larger than the uncorrelated emittance which comes in favor of decreasing the space charge effect.

Electrons within the cathode/anode gap can limit further emission of electrons from the surface of the photocathode due to space charge forces. This is known as the space charge current limitation [5, 6]. In this paper we investigate whether the space charge current limitation depends on the magnetization of the electron beam. Further, in a bunch, Coulomb repulsive forces mainly depend on the bunch size. Also, according to Child-Langmuir law the space charge current limitation depends on the gun voltage. Hence, the space charge current limitation behavior of a magnetized electron beam was investigated as a function of laser size at the photo-cathode, laser pulse width, and gun voltage and compared with the non-magnetized beam.

EXPERIMENTAL METHOD

Average beam current was measured at the dump by changing the laser power at the photocathode for different cathode solenoid currents (0, 100, and 200 A). This procedure was repeated using a variety of laser spot sizes at the cathode (1.00, 0.50, and 0.25 mm), laser pulse widths (120, 70, and 1 ps) and gun voltages (200, 150, and 100 kV), for magnetized and non-magnetized beam. The photocathode QE represents the ratio of emitted electrons to incident photons as:

$$QE = \frac{hc I}{\lambda e P} \times 100\% = \frac{124}{\lambda} \frac{I}{P} \% \quad (4)$$

where P (W) is the incident laser power, I (mA) is the measured average current, λ is the laser wavelength (515 nm), h is Planck's constant (6.626×10^{-34} Js), e is the electron charge (1.602×10^{-19} C), and c is the speed of light (2.998×10^8 m/s). Bunch charge is determined by dividing the measured average beam current by the bunch repetition rate.

SIMULATIONS

GPT was used to model the beamline [7]. Simulation was performed using measurement parameters of each configuration by changing the initial bunch charge from pC to few nC and by tracking the delivered charge at the dump. The 3D electric field map of the photo-gun generated by CST Studio Suite and 2D magnetic field map of the cathode solenoid generated from Opera software were implemented to generate more realistic simulations [8]. The beam line solenoids with their field maps and beam pipe radii throughout the beamline were also included. The GDFMGO solver program of GPT was used for corrector optimization to maximize charge extraction. Further, a gray-scale bitmap image of the laser profile weighted with the QE profile was implemented as the initial particle distribution since all the laser spots were not proper Gaussian in

profile. Figure 2 shows the laser distribution of 1.64 mm (rms) size, QE image and the initial particle distribution.

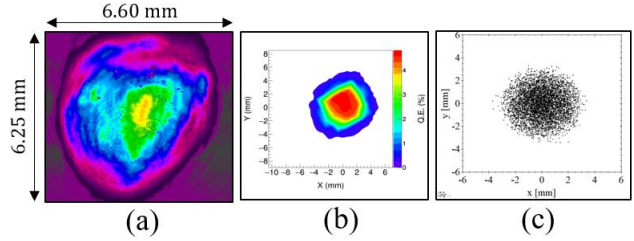


Figure 2: (a) Laser profile, (b) QE profile, and (c) Initial particle distribution.

RESULTS

Figure 3 illustrates the delivered charge at the dump as a function of the initial bunch charge (calculated from incident laser pulse energy and QE) and the corresponding GPT simulations for different cathode solenoid currents.

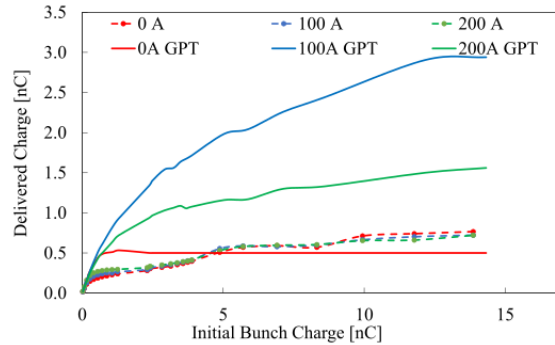


Figure 3: Delivered charge at the dump vs initial bunch charge for 0, 100 and 200 A cathode solenoid currents (225 kV, 50 kHz, 75 ps (FWHM), 1.64 mm (rms)).

The space charge limit is reached at ~ 0.3 nC and increased for a maximum extracted charge of 0.7 nC. We also see a less notable effect of magnetization on the space charge current limitation at small initial bunch charges. However, the charge beyond ~ 0.3 nC is likely to originate from the edge of the Gaussian laser profile. Also, we believe that the oscillatory behaviour seen at higher pulse energies likely stems from beam loss. The limited beamline aperture and insufficient strength of the focusing solenoids prevent clean transportation of the beam to the dump [9]. GPT simulations show some agreement at 0 A, but a large discrepancy at 100 A and 200 A which will discuss in next section. Further, GPT does not show any notable effect of magnetization on the space charge current limitation.

Figure 4 summarizes measurement versus GPT simulation on how the magnetization affect the space charge current limitation as a function of gun high voltage, laser spot size, and laser pulse width. These plots show the expected results, namely higher gun voltage permits the delivery of higher bunch charge beam. Moreover, they agree with what is expected from the Coulomb repulsive force where, by increasing the bunch dimensions, the space charge force can be suppressed to increase the extracted charge.

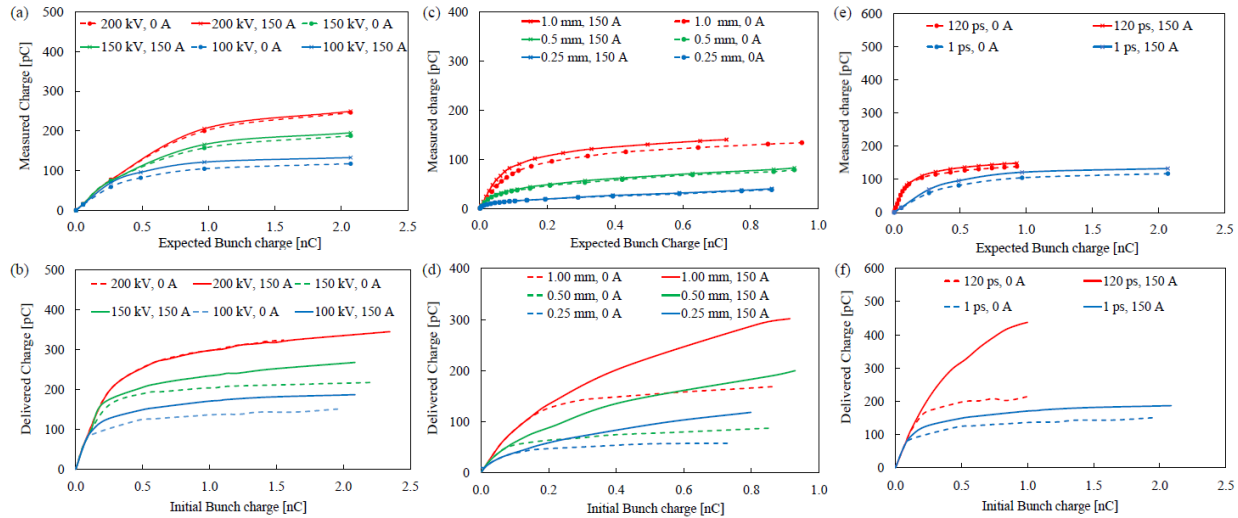


Figure 4: (a) Measured charge vs expected bunch charge and (b) corresponding GPT simulations for different gun high voltages for magnetized and non-magnetized beam (50 kHz, 1 ps, 1.54 mm (rms)). (c) Measured charge vs expected bunch charge and (d) corresponding GPT simulations for different laser spot sizes for magnetized and non-magnetized beam (100 kV, 50 kHz, 70 ps (FWHM)). (e) Measured charge vs expected bunch charge and (f) corresponding GPT simulations for different laser pulse widths for magnetized and non-magnetized beam (100 kV, 50 kHz, 1.54 mm (rms)).

The GPT simulation follows the same trend but shows higher charge extraction from the magnetized beam than the non-magnetized one. However, both measurements and simulations indicate a less notable effect of magnetization on space charge current limitation.

SIMULATION RESULTS ANALYSIS

Although GPT does not show any notable effect of magnetization on space charge current limitation, it shows higher beam extraction achievable for magnetized beam than for non-magnetized beam. This is mainly because the cathode solenoid focuses the beam from the beginning of beam flight that minimizes the beam loss. Nevertheless, as depicted in Figure 3, much higher beam extraction estimated for cathode solenoid current at 100 A than at 200 A, because of mismatch oscillation that resulted from non-uniform cathode magnetic field [8]. Thus, the beam size is smaller in 100 A case than in 200 A case, and the beam loss varies accordingly. Figure 5 illustrates the simulated beam loss along the beamline for 0 A, 100 A and 200 A cathode solenoid currents.

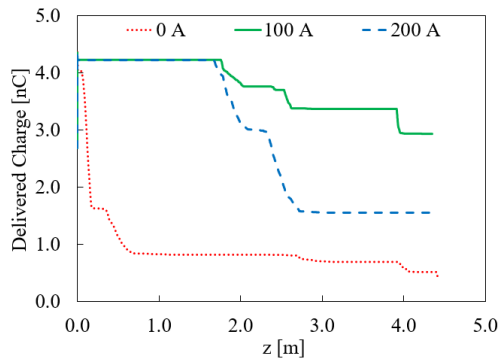


Figure 5: Beam loss along the beamline.

CONCLUSION

In summary, Jefferson Lab's new compact DC high voltage photo-gun and beamline were used to investigate the space charge effect in magnetized electron beam. Measurements were taken by varying the laser power and tracking the average current at the dump for different cathode solenoid currents. Further, these measurements were repeated for different gun high voltages, laser spot sizes and laser pulse widths. GPT simulation was performed for all measurements. Both measurements and simulation showed that there is little notable effect of magnetization on space charge current limitation. In addition, both agreed that the space charge current limitation can be reduced by using a higher gun voltage with larger laser spot size at the cathode and longer pulse width, regardless of the beam being magnetized. The limited beamline aperture and insufficient strength of the focusing solenoids caused the major beam loss. GPT simulation indicated that more beam could be extracted with magnetized beam than the non-magnetized beam because of the cathode solenoid focusing. Further, we found that the beam loss also depends on the cathode solenoid current due to the mismatch oscillation caused by the non-uniform cathode magnetic field.

ACKNOWLEDGEMENTS

This work is supported by the Department of Energy, under contract DE-AC05-06OR23177 and the Laboratory Directed Research and Development program.

REFERENCES

[1] Y. Derbenev and A. Skrinsky, "Magnetization effect in electron cooling," *Fiz.Plazmy*, vol. 4, p. 492, 1978. [*Sov.J. Plasma Phys.* 4, 273 (1978)].

- [2] R. Brinkmann, Y. Derbenev and K. Flöttmann, “A low emittance flat-beam electron source for linear colliders,” *Phy. Rev. ST Accel. Beams*, vol. 4, p. 053501, 2001.
- [3] S. Zhang et al., “High current high charge magnetized and bunched electron beam from a DC photogun for JLEIC cooler”, in *Proc. 10th Int. Particle Accelerator Conf. (IPAC’19)*, Melbourne, Australia, 2019.
- [4] M. Reiser, *Theory and Design of Charged Particle Beams*. New York, USA: Wiley-VCH, 2008. [2] R. Brinkmann, Y. Derbenev and K. Flöttmann, “A low emittance flat-beam electron source for linear colliders,” *Phy. Rev. ST Accel. Beams*, vol. 4, p. 053501, 2001.
- [5] M. Migliorati M. Ferrario and L. Palumbo, “Space charge effects”, *Proc. CAS-CERN Accelerator School*, Geneva, 2014.
- [6] I. Langmuir, “The effect of space charge and residual gases on thermionic currents in high vacuum”, *Phys. Rev.*, vol. 2, p. 450–486, 1913.
- [7] General Particle Tracer, <http://www.pulsar.nl/gpt>
- [8] S.A.K. Wijethunga et al., “Simulation study of the magnetized electron beam”, in *Proc. 9th Int. Particle Accelerator Conf. (IPAC’18)*, Vancouver, Canada, 2018.
- [9] S.A.K. Wijethunga et al., “Space charge study of the Jefferson Lab magnetized electron beam”, in *Proc. North American Particle Acc. Conf. (NAPAC’19)*, Lansing, MI, USA, 2019.